

Efficient Inscription of High Quality FBGs on ZBLAN Fiber With a Femtosecond Laser

Rui Liu, Zilun Luo, Luping Wu, Jianjun Ran, Yuji Wang, Cailiang Lv, Shiqin Qin, Zhiyong Bai , Ying Wang , Shen Liu , Changrui Liao , *Member, IEEE*, and Yiping Wang , *Senior Member, IEEE*

Abstract—An efficient inscription method for low insertion loss fiber Bragg gratings in ZBLAN fiber is presented, and the effects of femtosecond laser with different pulse numbers and repetition rate on the morphology of the refractive index modulation region and the insertion loss of ZBLAN fiber gratings were investigated. It is experimentally proved that the thermal effect of multiple pulses of high repetition rate femtosecond lasers avoid the generation of microcracks in the process of grating preparation, which greatly reduces the insertion loss. At the same time, the efficiency of grating inscription was greatly improved by utilizing the spherical aberration, the self-focusing effect in ZBLAN fiber and the parallel inscription technique. Finally, a parallel-integrated fiber Bragg grating consisting of three fiber Bragg gratings was inscribed on a ZBLAN fiber in 2.5 minutes by using 1 MHz femtosecond laser burst mode with a reflectivity of 99.6% and an insertion loss of only 0.1 dB, and the temperature sensitivity of this FBG was tested to be 26.17 pm/°C.

Index Terms—Fiber Bragg grating, laser material processing, mid-infrared, ZBLAN fiber.

Received 20 November 2024; revised 6 January 2025; accepted 14 January 2025. Date of publication 17 January 2025; date of current version 2 May 2025. This work was supported in part by the National Natural Science Foundation of China under Grant 62275169, Grant 62122057, and Grant 62275172, in part by the Natural Science Foundation of Guangdong Province under Grant 2022A1515010183 and Grant 2023A1515010753, in part by the Science, Technology and Innovation Commission of Shenzhen Municipality under Grant KQTD20221101093605019 and Grant JCYJ20210324120403009, and in part by the Ling Chuang Research Project of China National Nuclear Corporation. (Corresponding author: Zhiyong Bai.)

Rui Liu, Zilun Luo, Luping Wu, Jianjun Ran, Yuji Wang, Cailiang Lv, Shiqin Qin, Zhiyong Bai, Ying Wang, Shen Liu, and Changrui Liao are with the Shenzhen Key Laboratory of Photonic Devices and Sensing Systems for Internet of Things, Guangdong and Hong Kong Joint Research Centre for Optical Fibre Sensors, State Key Laboratory of Radio Frequency Heterogeneous Integration, Shenzhen University, Shenzhen 518060, China, and also with the Shenzhen Key Laboratory of Ultrafast Laser Micro/Nano Manufacturing, Key Laboratory of Optoelectronic Devices and Systems of Ministry of Education/Guangdong Province, College of Physics and Optoelectronic Engineering, Shenzhen University, Shenzhen 518060, China (e-mail: 2060453053@email.szu.edu.cn; luozhilun2022@email.szu.edu.cn; wuluping2020@email.szu.edu.cn; 2100453055@email.szu.edu.cn; 2042591190@qq.com; 2300453024@email.szu.edu.cn; 2310452082@email.szu.edu.cn; baizhiyong@szu.edu.cn; yingwang@szu.edu.cn; shenliu@szu.edu.cn; cliao@szu.edu.cn).

Yiping Wang is with the Shenzhen Key Laboratory of Photonic Devices and Sensing Systems for Internet of Things, Guangdong and Hong Kong Joint Research Centre for Optical Fibre Sensors, State Key Laboratory of Radio Frequency Heterogeneous Integration, Shenzhen University, Shenzhen 518060, China, also with the Shenzhen Key Laboratory of Ultrafast Laser Micro/Nano Manufacturing, Key Laboratory of Optoelectronic Devices and Systems of Ministry of Education/Guangdong Province, College of Physics and Optoelectronic Engineering, Shenzhen University, Shenzhen 518060, China, and also with the Guangdong Laboratory of Artificial Intelligence and Digital Economy (SZ), Shenzhen 518107, China (e-mail: ypwang@szu.edu.cn).

Color versions of one or more figures in this article are available at <https://doi.org/10.1109/JLT.2025.3531007>.

Digital Object Identifier 10.1109/JLT.2025.3531007

0733-8724 © 2025 IEEE. All rights reserved, including rights for text and data mining, and training of artificial intelligence and similar technologies. Personal use is permitted, but republication/redistribution requires IEEE permission. See <https://www.ieee.org/publications/rights/index.html> for more information.

I. INTRODUCTION

IN RECENT years, mid-infrared lasers have been employed extensively in a variety of research fields including healthcare [1], atmospheric communication [2], molecular detection [3], etc., because of the location in the atmospheric window and molecular vibration spectral region. In particular, as cavity mirrors, fiber Bragg gratings (FBGs) constitute integral components of mid-infrared fiber lasers [4], [5], [6], and their inscription techniques are crucial and widely studied. So far, different inscription methods have been explored and applied to many different types of mid-infrared fibers [7], [8], [9], [10], [11], [12], [13], [14], [15], [16], [17].

In the beginning, FBG in ZBLAN fiber were processed by using UV laser with conventional holographic interferometry [7] or through phase mask [8]. At this time, because ZBLAN fiber is not photosensitive, additional rare earth elements like cerium need to be added to it, moreover, it exhibits a limited refractive index modulation and possesses low thermal stability and laser damage threshold. In contrast, femtosecond (fs) laser modulation takes advantage of the nonlinear absorption of the material, does not require additional material sensitization, and has become the most popular fiber grating preparation technique by virtue of its higher refractive index modulation and better stability of the modulation. In 2007, Bernier et al. [9] inscribed FBG in non-photosensitized ZBLAN fiber by using fs laser pulses and a phase mask for the first time, but the coating of the fiber had to be removed before fabricating, which reduced mechanical strength of the fiber. In 2018, they wrote FBGs in an erbium-doped fluoride glass fiber without removing the polymer coating, achieving a maximum laser output power of 41.6 W at 2824 nm [10]. However, using phase mask for FBG preparation limit ability to flexibly adjust the resonant wavelength of grating. Comparatively, fs laser direct writing techniques have solved this problem, including point-by-point [11], [12], line-by-line [13], [14], and plane-by-plane [15], [16], [17] methods, that is, through the displacement platform to achieve point, line or plane of the periodic modulation region to form a grating. Among them, the line-by-line and plane-by-plane methods have uniform modulation area, and the insertion loss of the FBG is low, but they need to scan in multiple directions, which take longer time. The point-by-point method is exactly the opposite, the preparation efficiency is high, but the inscribed FBG generally has a significant insertion loss. So far, it is difficult to maintain a high writing efficiency of FBG in ZBLAN fibers while ensuring very low insertion loss and high reflectivity.

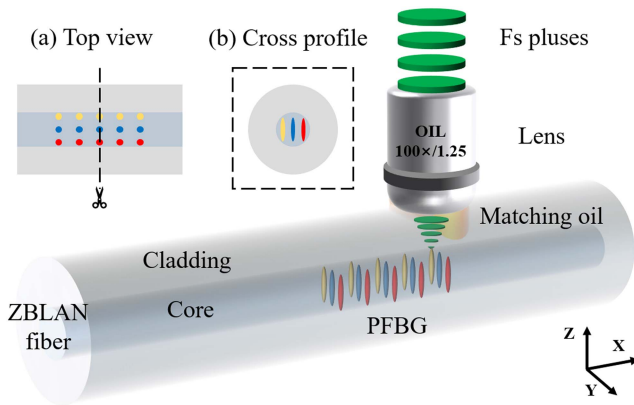


Fig. 1. Schematic of the FBG fabricated by fs laser on ZBLAN fiber. (Insets: (a) Top view and (b) cross-profile schematic of a PI-FBG consists of three FBGs).

In this letter, we proposed a low insertion loss parallel-integrated fiber Bragg grating (PI-FBG) [18] that simultaneously meets very high preparation efficiency and very low insertion loss by using burst mode method and parallel inscribe method. The thermal effect due to the high repetition rate and the multi-pulse of burst mode results in a uniform modulation area and thus guarantees a relatively low insertion loss (IL). And the spherical aberration caused by the multilayer structure of the ZBLAN fiber, the self-focusing effect of the femtosecond laser in the fiber and the thermal diffusion effect will make the refractive index modulation region show an ellipsoidal distribution, increasing the volume of the modulation region, and further reducing the insertion loss of the fiber grating. At the same time, combined with the parallel inscription technology, high-efficiency grating inscription can be realized, PI-FBG with reflectivity up to 99.6% can be inscribed within 2.5 minutes, and the insertion loss is only 0.1 dB.

II. PROCESS AND PRINCIPLE

The ZBLAN fiber (Le Verre Fluoré) used in our experiment with core and cladding diameters of $6.5 \mu\text{m}$ and $125 \mu\text{m}$, respectively, and the numerical aperture (NA) is 0.23. An fs laser with a wavelength of 515 nm, a pulse width of 290 fs, and a repetition rate of 1 MHz was employed. As shown in Fig. 1, the pulses were focused by a $100\times$ Leica oil-immersion objective with a NA of 1.25, and form a modulation in the ZBLAN fiber core. The detailed inscription process is as follows: firstly, the ZBLAN fiber was clamped by a pair of fiber holders mounted on a three-dimensional air flotation stage, and the fs laser beam was focused into the center of the fiber core. The axial direction of the fiber and the incident direction of laser beam are parallel to the x-axis and the z-axis of the translation stage, respectively. Secondly, by programmatically controlling the stage, the optical fiber is periodically moved along the x-axis, with each period modulated by multiple femtosecond pulses, go back to the starting point, move the y-axis to $1.5 \mu\text{m}$ left and right the FBG just written, and repeat the second step to prepare the second and third FBGs. And the top view and the cross-profile schematic of inscribed FBG are shown in the inset (a) and (b) in

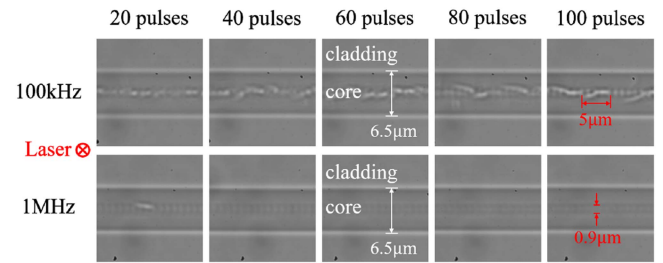


Fig. 2. Top view microscope images of refractive index modulations regions induced by using different pulse repetition rate (i.e., 1 MHz and 100 kHz) and various number of pulses (i.e., 20, 40, 60, 80 and 100).

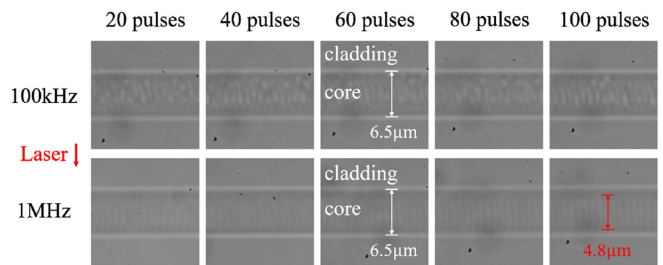


Fig. 3. Lateral view microscope images of refractive index modulations regions induced by using different pulse repetition rate (i.e., 1 MHz and 100 kHz) and various number of pulses (i.e., 20, 40, 60, 80 and 100).

Fig. 1, respectively. The entire preparation process is controlled in less than 2.5 minutes.

Fig. 2 shows the top view microscope images of FBGs modulated with 20, 40, 60, 80 and 100 pulses per period based on 100 kHz and 1 MHz repetition rate, respectively. And the energy of each pulse was 40.3 nJ. As can be seen from the figure, when the repetition rate of laser is 100 kHz, cracks appear in the laser modulation region, and the size of the cracks increases as the number of pulses increased. When the number reaches 100, the size of the crack is about $5 \mu\text{m}$. It is clear that the situation improved significantly when the pulse repetition frequency is 1 MHz. There are only a few cracks in the modulation region at a pulse number of 20, and when the pulse number is further increased, cracks no longer appeared and the morphology did not change much, but only became slightly darker. The size of a single modulation point is about $0.9 \mu\text{m}$ in diameter. Typical glass thermal diffusion time are on the order of μs , and at low repetition rate there is enough time for the deposited heat to diffuse out before subsequent pulses arrive. But this can lead to cracks appearing due to the large thermal expansion coefficient ($17.2 \times 10^{-6} \text{K}^{-1}$) and low fracture toughness ($0.32 \text{MPa m}^{1/2}$) of ZBLAN. At the same time, the glass transition temperature T_g of ZBLAN is $265 \text{ }^\circ\text{C}$, at high repetition rate, heat will accumulate and the temperature near the focal point will be higher than T_g , the modulation region undergoes a process of melting and re-solidification. And due to isotropic heat diffusion, the refractive index changes in the modulation region are very uniform, and cracks do not occur [19], [20], [21], [22], [23].

Fig. 3 show the corresponding Lateral view microscope images of Fig. 2. From the lateral view, when the pulse repetition

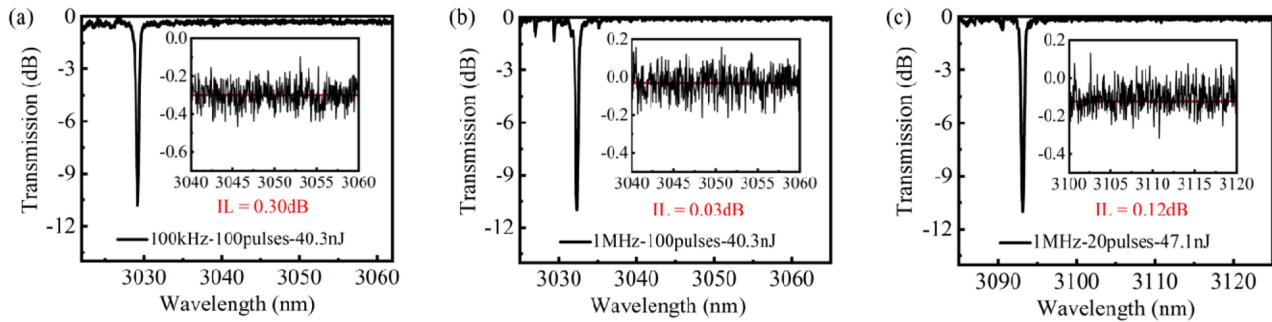


Fig. 4. Transmission spectra of FBGs modulated with (a) 100 kHz pulses repetition rate, 100 pulses per period and 40.3 nJ per pulse, (b) 1 MHz pulses repetition rate, 100 pulses per period and 40.3 nJ per pulse, (c) 1 MHz pulses repetition rate, 20 pulses per period and 47.1 nJ per pulse, respectively.

rate is 100 kHz, similar to the cracks in the top view, no matter how many pulses it is, there are so many uneven bright spots in the modulation region that the periodicity of the grating is affected. Relatively, when the repetition rate is 1 MHz, the lateral view of the modulation region looks uniform with well-defined periods whether the number of pulses is 20, 40, 60, 80 or 100. This is also attributed to the aforementioned thermal effect of multiple pulses at high repetition rate. The modulation region length is $4.8 \mu\text{m}$, which covers almost the entire fiber core (also for 100 kHz). This is due to the fact that we wrote the grating with out removing the coating layer of the ZBLAN fiber, and the multilayer structure of the fiber introduces aberration, making the focal point elongated vertically [12]. In addition, the self-focusing effect induced at high peak power of the fs laser pulse and the thermal effect at high repetition rate will also lead to the elongation [21], [24], [25].

III. EXPERIMENTS AND RESULTS

To more intuitively compare the modulation effect of different parameters on FBG quality, we selected FBGs inscribed with 100 kHz&100 pulses, 1 MHz&100 pulses and 1 MHz&20 pulses for spectral comparison. In addition, in order to compare the IL at a same dip resonance, the first two FBGs were inscribed with a single pulse energy of 40.3 nJ, and the third FBG was inscribed with a single pulse energy of 47.1 nJ. By the way, the pitch of this three FBGs are 1.027, 1.028 and $1.049 \mu\text{m}$. We tested the spectra responses of these FBGs using an ultra-broadband light source (LEUKOS, MIR 4.8) and a spectrometer (YOKOGAWA, AQ6377) in the mid-infrared wavelength band. The two ends of the ZBLAN fiber are cut flat and connected to the light source and spectrometer respectively through a bare fiber terminator, and the spectrum of the light source is subtracted in advance before the grating is inscribed in order to facilitate the analysis of the IL introduced by the femtosecond laser modulation. The test results are shown in Fig. 4. According to the results, the attenuations of Bragg resonance of these three FBGs are almost the same (i.e., 10.81, 10.97 and 10.98 dB), located at 3029.2, 3032.3 and 3079.9 nm, the 3 dB bandwidths are 0.64, 0.58 and 0.62 nm, and the ILs are 0.30, 0.03 and 0.12 dB, respectively. It is worth noting that the second FBG inscribed by 100 pulses with 1 MHz repetition rate and 40.3 nJ single pulse energy has

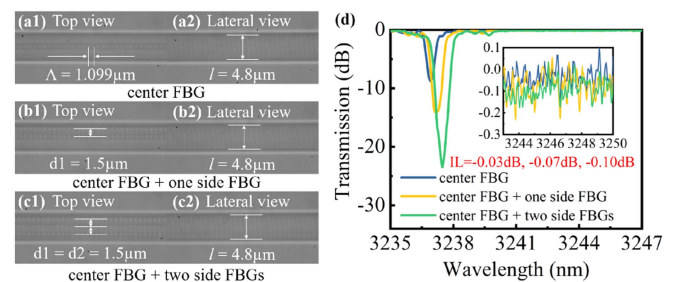


Fig. 5. The microscopic images of the inscription process of PI-FBG. (a1) The top view and (a2) lateral view microscopic images of the center FBG; (b1) (b2) for the center FBG and one side FBG; (c1) (c2) for the center FBG and two side FBGs; (d) the spectra of the inscription process of PI-FBG.

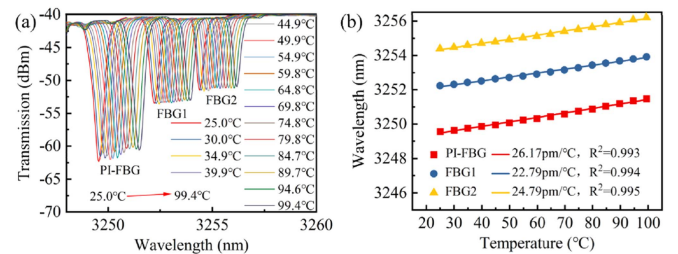


Fig. 6. (a) Temperature tuning spectra of PI-FBG, FBG1 utilized the thermal effect and FBG2 inscribed without thermal effect and (b) corresponding temperature characteristic curves and fitting.

the smallest IL, which is 1/10 and 1/4 of that of the first and the third FBG, respectively. It proves that it is feasible to reduce the IL of a FBG by using the thermal effect, and it requires not only a high repetition rate of fs pulses, but also the modulation of a large number of pulses per period.

Therefore, we chose a 1 MHz repetition frequency, 100 pulses per cycle, and a single pulse energy of 40.3 nJ to prepare FBGs. At the same time, in order to allow the refractive index modulation region to cover the fiber core in another dimension as well, while guaranteeing a high writing rate, we adopt a parallel integrated writing method. The FBG prepared by this method is called PI-FBG. Fig. 5 has shown the process of the PI-FBG inscription. The inscribing process is as follows, firstly, the optical axis of the fiber is adjusted to be parallel to the x-axis

TABLE I
COMPARISON OF LENGTH, WRITING TIME, REFLECTIVITY AND INSERTION LOSS OF MID-INFRARED FIBER GRATINGS WRITTEN BY DIFFERENT WRITING METHODS

Fiber	Method	Length /mm	Processing time	Reflective /%	κ/m^{-1}	Insertion loss /dB	Reference
ZBLAN	Point by point	20	-	48.7	43.2	0.17	[12]
			-	98.4	137	-	
Fluorotellurite Fiber	Shell-like period	5	<30s	>99	599	1.5	[13]
Ho ³⁺ /Pr ³⁺ : AlF ₃	Line by line	8	-	98.9	368	1	[14]
Ho ³⁺ /Pr ³⁺ : ZBLAN	Plane by plane	15	2h	~50	58.8	-	[15]
ZBLAN	Single pass		2.5h	90.1	368	0.09	[17]
	Double pass	5	5h	92.6	395	0.12	
	Stacking		7h	96.2	464	0.17	
ZBLAN	PI-FBG	10	2.5min	99.6	345	0.10	This work

movement direction of the stage to ensure that the inscribed FBG is in the middle of the fiber core, and then it starts to move the x -axis cyclically to form the center FBG. As shown in Fig. 5(a1) and (a2), the inscribed FBG is indeed in the center of the core, both in the top view and the lateral view. The depth of the modulation region is $4.8 \mu\text{m}$. The FBG has a pitch of $1.099 \mu\text{m}$, a length of 10 mm with x -axis travel speed of 0.2 mm/s, and its inscription took 50 s only. The depth of the modulation region is $4.8 \mu\text{m}$. The FBG has a pitch of $1.099 \mu\text{m}$, a length of 10 mm with x -axis travel speed of 0.2 mm/s, and its inscription took 50s only. The corresponding FBG transmission spectrum is shown as the blue line in Fig. 5(d), whose Bragg resonance dip is located at 3236.9 nm with a depth of -8.79 dB, and the IL is 0.03 dB. After inscribing the first grating, the displacement stage is controlled to return to its starting point, and the fiber is moved $1.5 \mu\text{m}$ in the negative direction of the y -axis, and this point is used as the starting point for the inscription of the second FBG. As shown in Fig. 4(b1), the second FBG is located at $1.5 \mu\text{m}$ above the center FBG in the top views. The corresponding grating transmission spectrum is shown as the yellow line in Fig. 4(d), located at 3237.2 nm with a dip depth of -14.12 dB, and the IL is up to 0.07 dB. Then repeat the steps to fabricate the third FBG $1.5 \mu\text{m}$ below the center FBG in the top view. In the end, the PI-FBG, consisting of three FBGs, was inscribed, which only took 2.5 minutes. The final spectrum of PI-FBG is shown as the green line in Fig. 4(d), which is located at 3237.5 nm with a dip depth of -23.46 dB, i.e., the reflectivity of the PI-FBG reaches 99.6%, and the IL is still only 0.10 dB. By utilizing the parallel inscription techniques, modulation region covering almost the entire fiber core is achieved in each period. Overall, the method achieved plane-by-plane modulation with the efficiency of the point-by-point approach.

Table I lists some data on the length, inscription time, reflectivity, coupling coefficient and insertion loss of FBGs inscribed in various ways, which are typical values in the respective articles. We can find that the point-by-point modulation will lead to larger insertion loss, such as in reference [12], the reflectivity of the grating written point-by-point method is only 48.7% and its IL

reaches 0.17 dB. In reference [13], the shell-like period method is the single pulse point-by-point method to get the line-by-line modulation, which took less than 30 seconds to fabricate a 5 mm long FBG, but the IL was up to -1.5 dB. Conversely, the line-by-line and plane-by-plane modulation may have smaller IL but they took longer time. Reference [14] used the line-by-line method, and it took 1 hour to fabricate an 8 mm long FBG, and in reference [15], it took 2 hours to fabricate a 15 mm long FBG using the plane-by-plane method. In reference [17], it took 2.5 hours, 5 hours and 7 hours to realize the line-by-line modulation by single pass and double pass, and the plane-by-plane modulation by stacking, respectively. With the method in this letter, a grating with IL of only 0.10 dB and reflectivity of 99.6% can be realized in 2.5 minutes, with an efficiency similar to the point-by-point method, and a grating coupling coefficient similar to that of the line-by-line and plane-by-plane methods, which, in comparison, should be the optimal means of FBG fabricating at present.

A change in the external temperature leads to a change in the resonant wavelength of the FBG, and this can be utilized to achieve tuning of the laser output wavelength. In order to investigate the temperature characteristics of PI-FBGs, we inscribed PI-FBG, FBG1 that utilized the thermal effect and FBG2 that did not utilize the thermal effect on ZBLAN fibers and tested them simultaneously for temperature. The length of PI-FBG, FBG1 and FBG2 is both 10 mm, the interval between FBGs is 20 mm, and the resonance wavelengths of FBGs at room temperature are 3249.5 nm, 3252.2 nm and 3254.4 nm, respectively. We placed the ZBLAN fiber with the three kinds of gratings inscribed into a temperature oven, starting at room temperature in 5°C one step, and recorded the spectra as they stabilized at the current temperature, until the oven approached nearly 100°C . As shown in Fig. 5(a), the spectral curves of PI-FBG, FBG1 and FBG2 are all red-shifted with increasing temperature, and the red shift magnitude is approximately the same. The values of the wavelengths corresponding to the lowest point of the curve at each temperature for the three gratings were selected and used to plot the wavelength versus temperature

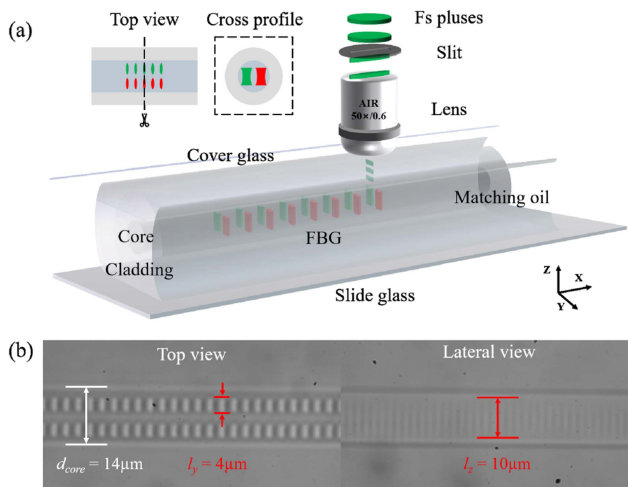


Fig. 7. (a) Schematic of the FBG inscribed by fs laser on large core diameter ZBLAN fiber. (b) Corresponding top view and lateral view microscope images of PI-FBG.

curves and fit them linearly. The results are shown in Fig. 5(b), where it can be seen that the temperature sensitivity of PI-FBG, FBG1 and FBG2 are 26.17 pm/°C, 22.79 pm/°C and 24.79 pm/°C, respectively, corresponding to R^2 of 0.993, 0.994 and 0.995, respectively. The difference in temperature sensitivity between PI-FBG and FBG1 probably because that PI-FBG contains two FBGs that are closer to the cladding, and thus are slightly more sensitive to external temperature changes. While the difference in temperature sensitivity between FBG1 and FBG2 may come from the difference between athermal modulation and thermal modulation.

Finally, we considered that when the fiber core size is larger, the highest efficiency cannot be achieved if we still use only the parallel integration method, for which we further explore the combination of other means. As shown in Fig. 7(a), the oil-immersion objective was replaced with an air objective, and added a cover glass above the ZBLAN fiber to further widen its spherical aberration and thus elongate the length of the focused spot in the z-axis. In addition, the length of the focused spot in the y-axis can also be elongated by adding a slit (or a pair of cylindrical lenses) in front of the objective [26]. These modifications result in a larger modulation region. Fig. 7(b) and (c) are the top and lateral view microscope images of the modulation region in a large core diameter ZBLAN fiber (14/250) using this method and parallel integrated fabricating technique. The length of the modulation region in the y-axis and z-axis is 4 μm and 10 μm respectively. The PI-FBG consisting of two FBGs can basically cover the entire fiber core. Using this method (or adding a spatial light modulator in the optical path for direct parallel processing) can further improve the FBG fabricating efficiency.

IV. CONCLUSION

In this work, a highly efficient method for fabricating low insertion loss mid-infrared fiber gratings is proposed, which utilizes the thermal effect of high-frequency fs laser multi-pulses

to achieve thermal modulation of ZBLAN fibers, thus reducing insertion loss. Meanwhile, by utilizing the spherical aberration, the self-focusing effect and the parallel inscribing process, the plane-by-plane modulated grating is achieved, which further reduces the insertion loss and enhances the FBG inscription efficiency at a very high level. Finally, we inscribed a PI-FBG consisting of three FBGs on a ZBLAN fiber in 2.5 minutes, achieving 99.6% reflectivity with an IL of 0.1 dB, and the temperature sensitivity of this type of PI-FBG was measured to be 26.17 pm/°C. By comparing other means of FBG inscription, the method used in this letter is perhaps the optimal means of inscribing high-quality mid-infrared FBGs at present, and the PI-FBGs inscribed by this method will have profound impact on the mid-infrared lasers, laying the foundation for further mid-infrared applications.

REFERENCES

- [1] M. A. Pleitez et al., "In vivo noninvasive monitoring of glucose concentration in human epidermis by mid-infrared pulsed photoacoustic spectroscopy," *Anal. Chem.*, vol. 85, no. 2, pp. 1013–1020, Dec. 2012, doi: [10.1021/ac302841f](https://doi.org/10.1021/ac302841f).
- [2] Z. Wang, B. Zhang, J. Liu, Y. Song, and H. Zhang, "Recent developments in mid-infrared fiber lasers: Status and challenges," *Opt. Laser Technol.*, vol. 132, Jul. 2020, Art. no. 10467, doi: [10.1016/j.optlastec.2020.106497](https://doi.org/10.1016/j.optlastec.2020.106497).
- [3] Q. Wang et al., "Dual-comb photothermal spectroscopy," *Nature Commun.*, vol. 13, Apr. 2022, Art. no. 2181, doi: [10.1038/s41467-022-29865-6](https://doi.org/10.1038/s41467-022-29865-6).
- [4] V. Fortin, M. Bernier, S. T. Bah, and R. Vallée, "30 W fluoride glass all-fiber laser at 2.94 μm ," *Opt. Lett.*, vol. 40, no. 12, pp. 2882–2885, Jun. 2015, doi: [10.1364/OL.40.002882](https://doi.org/10.1364/OL.40.002882).
- [5] F. Maes, V. Fortin, M. Bernier, and R. Vallée, "5.6 W monolithic fiber laser at 3.55 μm ," *Opt. Lett.*, vol. 42, no. 11, pp. 2054–2057, Jun. 2017, doi: [10.1364/OL.42.002054](https://doi.org/10.1364/OL.42.002054).
- [6] V. Fortin, F. Jobin, M. Larose, M. Bernier, and R. Vallée, "10-W-level monolithic dysprosium-doped fiber laser at 3.24 μm ," *Opt. Lett.*, vol. 44, no. 3, pp. 491–494, Feb. 2019, doi: [10.1364/OL.44.000491](https://doi.org/10.1364/OL.44.000491).
- [7] T. Taunay et al., "Ultraviolet-induced permanent Bragg gratings in cerium-doped ZBLAN glasses or optical fibers," *Opt. Lett.*, vol. 19, no. 17, pp. 1269–1271, Sep. 1994, doi: [10.1364/OL.19.001269](https://doi.org/10.1364/OL.19.001269).
- [8] M. Saad, L. R. Chen, and X. Gu, "Highly reflective fiber Bragg gratings inscribed in Ce/Tm Co-doped ZBLAN fibers," *IEEE Photon. Technol. Lett.*, vol. 25, no. 11, pp. 1066–1068, Jun. 2013, doi: [10.1109/LPT.2013.2258900](https://doi.org/10.1109/LPT.2013.2258900).
- [9] M. Bernier et al., "Bragg gratings photoinduced in ZBLAN fibers by femtosecond pulses at 800 nm," *Opt. Lett.*, vol. 32, no. 5, pp. 454–456, Mar. 2007, doi: [10.1364/OL.32.000454](https://doi.org/10.1364/OL.32.000454).
- [10] Y. O. Aydin, V. Fortin, R. Vallée, and M. Bernier, "Towards power scaling of 2.8 μm fiber lasers," *Opt. Lett.*, vol. 43, no. 18, pp. 4542–4545, Sep. 2018, doi: [10.1364/OL.43.004542](https://doi.org/10.1364/OL.43.004542).
- [11] D. D. Hudson, R. J. Williams, M. J. Withford, and S. D. Jackson, "Single-frequency fiber laser operating at 2.9 μm ," *Opt. Lett.*, vol. 38, no. 14, pp. 2388–2390, Jul. 2013, doi: [10.1364/OL.38.002388](https://doi.org/10.1364/OL.38.002388).
- [12] L. Chen et al., "High-quality fiber Bragg grating inscribed in ZBLAN fiber using femtosecond laser point-by-point technology," *Opt. Lett.*, vol. 47, no. 14, pp. 3435–3438, Jul. 2022, doi: [10.1364/OL.464006](https://doi.org/10.1364/OL.464006).
- [13] L. Liu et al., "Direct femtosecond laser inscription of an IR fluorotellurite fiber Bragg grating," *Opt. Lett.*, vol. 46, no. 19, pp. 4832–4835, Oct. 2021, doi: [10.1364/OL.439290](https://doi.org/10.1364/OL.439290).
- [14] N. Xu et al., "Direct femtosecond laser inscription of Bragg gratings in $\text{Ho}^{3+}/\text{Pr}^{3+}$ co-doped AlF_3 -based glass fibers for a 2.86 μm laser," *Opt. Lett.*, vol. 47, no. 3, pp. 597–600, Feb. 2022, doi: [10.1364/OL.448431](https://doi.org/10.1364/OL.448431).
- [15] G. Bharathan et al., "Direct inscription of Bragg gratings into coated fluoride fibers for widely tunable and robust mid-infrared lasers," *Opt. Exp.*, vol. 25, no. 24, pp. 30013–30019, Nov. 2017, doi: [10.1364/OE.25.030013](https://doi.org/10.1364/OE.25.030013).
- [16] K. Goya et al., "Plane-by-plane femtosecond laser inscription of first-order fiber Bragg gratings in fluoride glass fiber for in situ monitoring of lasing evolution," *Opt. Exp.*, vol. 26, no. 25, pp. 33305–33313, Dec. 2018, doi: [10.1364/OE.26.033305](https://doi.org/10.1364/OE.26.033305).

- [17] G. Bharathan et al., "Optimized laser-written ZBLAN fiber Bragg gratings with high reflectivity and low loss," *Opt. Lett.*, vol. 44, no. 2, pp. 423–426, Jan. 2019, doi: [10.1364/OL.44.000423](https://doi.org/10.1364/OL.44.000423).
- [18] Y. wang et al., "Parallel-integrated fiber Bragg gratings inscribed by femtosecond laser point by point technology," *J. Lightw. Technol.*, vol. 37, no. 10, pp. 2185–2193, May 2019, doi: [10.1109/JLT.2019.2899585](https://doi.org/10.1109/JLT.2019.2899585).
- [19] S. M. Eaton et al., "Heat accumulation effects in femtosecond laser-written waveguides with variable repetition rate," *Opt. Exp.*, vol. 12, no. 12, pp. 4708–4716, Jun. 2005, doi: [10.1364/OPEX.13.004708](https://doi.org/10.1364/OPEX.13.004708).
- [20] X. Zhu and N. Peyghambarian, "High-power ZBLAN glass fiber lasers: Review and prospect," *Adv. Optoelectron.*, vol. 2010, Mar. 2010, Art. no. 501956, doi: [10.1155/2010/501956](https://doi.org/10.1155/2010/501956).
- [21] S. Gross et al., "Ultrafast laser inscription in soft glasses: A comparative study of athermal and thermal processing regimes for guided wave optics," *Int. J. Appl. Glass Sci.*, vol. 3, no. 4, pp. 332–348, Nov. 2012, doi: [10.1111/ijag.12005](https://doi.org/10.1111/ijag.12005).
- [22] J. P. Bérubé, M. Bernier, and R. Vallée, "Femtosecond laser-induced refractive index modifications in fluoride glass," *Opt. Materials Exp.*, vol. 3, no. 5, pp. 598–611, Apr. 2013, doi: [10.1364/OME.3.000598](https://doi.org/10.1364/OME.3.000598).
- [23] A. Fuerbach et al., "Refractive index change mechanisms in different glasses induced by femtosecond laser irradiation," *Proc. SPIE*, vol. 9983, pp. 14–20, 2016, doi: [10.1117/12.2237368](https://doi.org/10.1117/12.2237368).
- [24] G. Fibich and A. L. Gaete, "Critical power for self-focusing in bulk media and in hollow waveguides," *Opt. Lett.*, vol. 25, no. 5, pp. 335–337, Mar. 2000, doi: [10.1364/OL.25.000335](https://doi.org/10.1364/OL.25.000335).
- [25] S.-H. Cho, H. Kumagai, and K. Midorikawa, "Fabrication of single-mode waveguide structure in optical multimode fluoride fibers using self-channeled plasma filaments excited by a femtosecond laser," *Appl. Phys. A*, vol. 77, pp. 359–362, Aug. 2003, doi: [10.1007/s00339-003-2157-x](https://doi.org/10.1007/s00339-003-2157-x).
- [26] J. He et al., "Femtosecond laser plane-by-plane inscription of Bragg gratings in sapphire fiber," *J. Lightw. Technol.*, vol. 41, no. 22, pp. 7014–7020, Nov. 2023, doi: [10.1109/JLT.2023.3294794](https://doi.org/10.1109/JLT.2023.3294794).

Rui Liu was born in Guangdong, China, in 1997. He received the B.Eng. degree in optoelectronic information science and engineering in 2020 from Shenzhen University, Shenzhen, China, where he is currently working toward the Doctoral degree in optical engineering. His research interests include optical fiber sensors and orbital angular momentum.

Zilun Luo was born in Guangdong, China, in 2000. He received the B.Eng. degree from optoelectronic information science and engineering in 2022 from Shenzhen University, Shenzhen, China, where he is currently working toward the M.S. degree in optical engineering. His research interests include optical fiber sensors and orbital angular momentum.

Luping Wu was born in Jiangxi, China, in 1998. He received the B.Eng. degree from the College of Information Engineering, Jiangxi University of Science and Technology, Ganzhou, China, in 2020. He is currently working toward the Ph.D. degree in optical engineering with Shenzhen University, Shenzhen, China. His research interests include optical fiber sensors and orbital angular momentum.

Jianjun Ran was born in Chongqing, China in 1996. He received the B.Eng. degree in optoelectronic information science and engineering from the Chongqing University of Technology, Chongqing, China, in 2020. He is currently working toward the Ph.D. degree in optical engineering with Shenzhen University, Shenzhen, China. His research interests include fiber optic sensors and orbital angular momentum.

Yuji Wang was born in Guangdong, China in 1999. He received the B.Eng. degree in 2022 from the College of Applied Technology, Shenzhen University, Shenzhen, China, where he is currently working toward the M.S. degree in optical engineering. His research interests include optical fiber sensors and orbital angular momentum.

Cailiang Lv was born in Guangdong, China in 2000. He received the bachelor's degree in engineering from the School of Physics and Electronic Engineering, Jiaying University, Meizhou, China, in 2023. He is currently working toward the master's degree in optical engineering with Shenzhen University, Shenzhen, China. His research focuses on fiber optic sensing.

Shiqin Qin was born in Guangxi, China, in 1998. She received the B.Eng. degree from the School of Electronic Engineering, Beijing University of Post and Telecommunications, Beijing, China, in 2020. She is currently working toward the master's degree in optical engineering with Shenzhen University, Shenzhen, China. Her research interests include optical fiber sensors and extreme environment sensing.

Zhiyong Bai received the Ph.D. degree in optics from Nankai University, Tianjin, China, in 2014. Since 2015, he has been with Shenzhen University, Shenzhen, China, as a Postdoctoral Research Fellow. Since 2018, he has been with Shenzhen University, as an Assistant Professor/Associate. His research interests include optical fiber gratings and orbital angular momentum.

Ying Wang received the Ph.D. degree in physical electronics from the Huazhong University of Science and Technology, Wuhan, China, in 2010. From 2009 to 2011, he was with Hong Kong Polytechnic University, Hong Kong, as a Postdoctoral Research Fellow. From 2011 to 2015, he has been with Wuhan Institute of Technology, Wuhan, as a Distinguished Professor. Since 2015, he has been with Shenzhen University, Shenzhen, China, as an Assistant Professor/Associate /Professor. His research interests include photonic crystal fibers and devices, and fiber optic biochemical sensing technology.

Shen Liu was born in Henan, China, in 1986. He received the B.E. degree in electronic and information engineering from PLA Air Force No.1 Aviation University, Changchun, China, in 2008, the M.S. degree in circuit and system from the Chongqing University of Posts and Telecommunications, Chongqing, China, in 2013, and the Ph.D. degree in optics from Shenzhen University, Shenzhen, China, in 2017. From 2017 to 2018, he was with Aston University, Birmingham, U.K., as a Postdoctoral Fellow. Since 2018, he has been with Shenzhen University as an Assistant Professor. He has authored or coauthored 11 patent applications and more than 90 journal and conference papers. His research interests include optical fiber sensors, WGMs resonator, and cavity optomechanics.

Changrui Liao (Member, IEEE) received the Ph.D. degree in electrical engineering from Hong Kong Polytechnic University, Hong Kong, in 2012. Since 2013, he has been with Shenzhen University, Shenzhen, China, as an Assistant Professor/Associate /Professor. His research interests include femtosecond laser micromachining, optical fiber sensors, and opto-microfluidics.

Yiping Wang (Senior Member, IEEE) received the Ph.D. degree in optical engineering from Chongqing University, Chongqing, China, in 2003. From 2003 to 2005, he was with Shanghai Jiao Tong University, Shanghai, China, as a Postdoctoral Fellow. From 2005 to 2007, he was with Hong Kong Polytechnic University, Hong Kong, as a Postdoctoral Fellow. From 2007 to 2009, he was with the Institute of Photonic Technology, Germany, as a Humboldt Research Fellow. From 2009 to 2011, he was with the Opto-Electronics Research Centre, University of Southampton, Southampton, U.K., as a Marie Curie Fellow. Since 2012, he has been with Shenzhen University, Shenzhen, China, as a Distinguished Professor. His research interests include optical fiber sensors, fiber gratings, and photonic crystal fibers. Prof. Wang is a Senior Member of the Optical Society of America and Chinese Optical Society.